

A Review of Side-lined Chunky Graphite Phenomena

H. Borgström and V. Furlakidis^{1*}

¹Department of Materials and Process Technology, Swerea SWECAST, Jönköping, Sweden

Considerable insight into Chunky graphite formation models and their corresponding mechanisms can be derived from revisiting graphite nucleation mechanisms in ductile iron. In particular, several unified theories related to the nucleation and growth of nodular graphite, need to be considered before Chunky graphite formation models and their corresponding mechanisms can be derived. This is justified by high resolution microscopy of quenching experiments, which elucidates that the formation of unwanted graphite forms like chunky occur shortly after graphite nucleation during eutectic solidification. Therefore it is the intension of this review to tie a number of nucleation theories stronger to events that have been shown to promote Chunky graphite formation. In particular a number of studies including radiography and spectroscopy will be reviewed that will shed new light into the Chunky graphite formation mechanism.

Keywords: Chunky graphite, ductile iron, nucleation.

Introduction

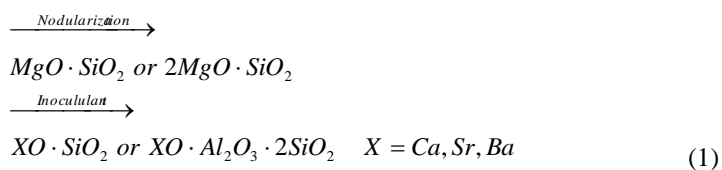
Even if certain in roads have been made in the understanding of Chunky graphite formation^{1,2,3,4,5,6} and control in ductile iron⁷, a systematic definition of remedies and adequate process control limits remain elusive. Furthermore, many times works on chunky graphite have been too complacent and too general in its execution. An example of this is how the role of Sb in the ductile iron microstructure has been investigated. The extensive use of Scanning electron microscopy is the reason for the lack of progress in describing the role of micro alloying components like Sb, which are commonly used to suppress Chunky Graphite if the right amount is used. Only with advanced auger electron spectroscopy is it possible to elucidate the 1-4 nm thin layer of Sb (and Sn) on the graphite nodule⁸. Furthermore, only a very few studies^{9,10,11} have addressed the development of the primary structure's morphology with respect to cooling rate and thermodynamic conditions. In addition, our understanding of the graphite nucleation mechanisms in ductile iron remains incomplete¹². This in turn is due to that there are several unified/alternative theories related to the nucleation and growth of nodular graphite, which need to be considered before Chunky graphite formation models and their corresponding mechanisms can be derived.

General overview of nucleation and growth of nodular graphite

The formation and development of precipitates, but also their lattice mismatch parameter with graphite in both nodularization and inoculation is what dictates whether nodular graphite will form^{7,13}. Experimentally it has been difficult to verify the theory, but later studies^{12,14} have included images of graphite nodule cross-sections with a clear 0.2 to 1µm MgO nuclei surrounded by MgS, CaS and Ca·Al₂O₃·SiO₂ precipitates. This implies that MgO forms first and provides a nucleating site for the later forming MgS and other precipitates¹².

There are also cases where no MgO has been observed¹⁵. Instead various precipitates/inclusions like sulphides, oxides, oxy-sulphides, silicates, nitrides have been found in graphite nodule centres¹⁵. The notable exception is carbides that have not been found in nodule centres but this is realistic owing to the fact that those oxides and sulphides are thermodynamically more stable¹⁵. The principal role of all these inclusions is to reduce the undercooling required for the heterogeneous nucleation, by e.g. reducing the lattice disregistry¹⁵

Central for the silicate theory¹⁵ is the reduction in lattice disregistry by formation events that occur during nodularization (i.e. Mg treatment) and inoculation, where the lattice disregistry constitutes a measure of the epitaxial fit between the nucleant particulate/inclusion and the graphite nodule. The main formation mechanism during the nodularization is the realization of Enstatite and Forsterite with reasonably high lattice disregistries of about 6 to 30% with graphite¹⁵ as seen in equation 1. *



*Corresponding author, email: henrik.borgstrom@swerea.se

These phases are then transformed into more faceted hexagonal silicate phases (seen in equation 1) during inoculation, yielding reduced lattice disregistries of about 1 to 8% with graphite¹⁵. The reduced lattice disregistries facilitate the formation of coherent/semi-coherent low energy interfaces between the nucleant and the graphite, which reduces the undercooling¹⁵. The implication of the silicate theory on Chunky graphite is tied to the coherency of the interfaces and the possible crystallographic growth direction of the nucleating graphite¹⁵, which is affected by the presence of trace elements¹⁵. In fact an excess amount of trace elements was found to increase the formation of detrimental type C inclusions in the graphite nodulus core during nodularization, which coincided with an increased amount of Chunky graphite^{13,15}. Here it is postulated that the impurities hinder the curved graphite growth necessary for graphite nodule formation in the austenite-liquid mushy zone, which has been discussed in view of chunky graphite formation.¹⁵ It is also believed that the formation of chunky graphite was tied to graphite growing with sufficient spheroidizing ability in the direction where the basal plane expands predominantly⁶. An example of what is believed to be the initial stages of Chunky graphite formation is when two Ca rich precipitates were close to the commonly found MgO nuclei in the graphite nodule centre¹⁶, had altered the solidification path of the graphite, which caused the graphite to branch out to chunky Graphite¹⁷.

In contrast to the silicate theory, there is in high purity Fe-C-Si systems a natural transition from plate like to nodular graphite morphologies¹⁵. If this is to occur the required purity for S is very high, but also entwined with a critical cooling rate. For slow (<40K/min), Intermediate (>40 K/min & <100K/min) and high (>100 K/min) cooling rates the required S purities are; 0.2 ppm, 1.5 ppm and 11 ppm, respectively^{15sic}. For these high purities no impurities could be found in the graphite nodule centres, in essence, favouring conditions for Gorschkov's gas bubble to prevail. Historically, Gorschkov's gas bubble theory has evolved into "the pore filling theory" by Karsay¹⁵ and finally into site theory proposed by Itofuji⁵. The theory postulates that graphite precipitates and grows inward into nodules on small pores/bubbles created during the nodulizing treatment⁵. A more elaborate description for the site theory^{6,9} dictates that unwanted graphite morphologies like Chunky graphite can be avoided if issues affecting the availability of enough Mg-gas bubbles are controlled during nucleation¹⁸. However, the occurrence of Mg-gas is highly questionable. Experimentally the pore filling effect has been observed after 12 hour dwells at 1150°C in a study on powder forging of Fe-C-Si¹⁹. Another study on liquid phase sintering of a similar Fe-C-Si system observed a partially graphite filled pore during a 90 min dwell at 1150°C in conjunction with cooling in vacuum, empowering the pore-filling effect²⁰. Noteworthy, is that in both these studies the impurity levels could be considered very low as gas atomized powders contain very small amounts of impurities²⁰.

Another mechanism occurring during the solidification process for ductile iron, is Vacancy Diffusion¹¹. This seems to occur when the austenite shell needs to deform plastically to grow around the graphite. Evidently wedge theory²¹ dictates that the plastic deformation of the austenite should directly cause Chunky Graphite. For this to occur, the chemical potential for the austenite and the graphite needs to be the same. However, situations have been elucidated where the austenite is in contact with the graphite without being able to form a shell, when the nodules are smaller than 14 microns^{11,22}. Here the underlying interface kinetics was affected when the graphite precipitated from the liquid.¹¹ This could cause defects in the graphite that changes its chemical potential during growth. Of particular interest is the combination of large growth rates and large interface kinetics when the nodules are small¹¹.

Generalized Chunky Graphite Formation Model

Chunky graphite formation models and mechanisms often built on quenching experiments and high resolution microscopy seem to agree on that the formation of unwanted graphite forms like chunky occur shortly after graphite nucleation during eutectic solidification⁹, even if there are discrepancies between the alternative theories. Theories proposed by Liu, Zhou and Gagné and Argo believe that the main chunky graphite formation mechanism is related to the dendrite growth of the austenite phase during solidification,^{1,3,4} It is also postulated that Chunky graphite is formed at the austenite/graphite interface, in the middle or at the end of the eutectic solidification before growing into the remnant liquid through a melt channel^{3,23}. The main steps of these models essentially entail:

1. *Spheroidal graphite precipitates and is surrounded by austenite shell*
2. *Spheroidal graphite nucleation finishes and chunky graphite precipitates at the austenite-residual melt interface.*
3. *Chunky graphite growth is fuelled by its thin channel connection with the residual melt.*

Discussion

The role of Graphite nodule core precipitates

In the first step, is it really enough to only consider the direct meta physics of the precipitating graphite and austenite? I believe that in order to make progress it is necessary to split the first mechanism into:

1. How does the graphite precipitate and grow?
2. How does the austenite develop?

The shortcomings in compounding the graphite and austenite became evident when one delves a little deeper into the mechanisms behind the silicate theory^{13,15}. In particular it is possible to question the nucleation of the silicates themselves. In an almost congruent way to *that graphite is a good nucleant to austenite, but austenite is a poor nucleant to graphite.*¹³ In particular, too little attention has been made to investigate the thermodynamic conditions surrounding the precipitation of the silicates independently from the nucleation of the graphite nodules. In the above treatment of the

silicate theory it is clear that the lattice mismatch of the silicates with respect to the graphite is reduced by successful inoculation. Furthermore, work on S has shown that sulphides can have both hexagonal and cubic structures¹⁰. For Sulphides having a hexagonal the unit cell structure it has been found that these can be good nucleation sites for graphite directly. However, small sulphides have been found encapsulated in silicates, which indicates that under certain conditions the unit cell structure for the sulphides could be a poor match for graphite, but a good one for silicates that are with proper treatment and inoculation good nucleation sites for graphite¹⁵. Further evidence of this is found in work on SiC additions to ductile iron, where it was demonstrated that the nucleation potential of the melt increased when the amount of silicates increased²⁴. It could well be that these studies presents an opening for understanding how to improve the inoculation and thus the nucleation of graphite during the latter part of the eutectic solidification, where evidently chunky graphite is precipitated.

Importance of Carbon Flootation

For the development of austenite dendrites the selection of a suitable carbon equivalent is critical since it is influenced by the alloying, dictates the melt viscosity, the risk for flotation, risk for carbide formation, the extent of micro-cavities, pearlite, carbides and denodularization etc. To avoid chunky graphite a slightly hypoeutectic composition is recommended for heavy sections⁷. Unfortunately, even if common logic would lead one to assume that graphite flotation would aggravate chunky graphite no specific study has been identified where this has been done systematically. However, the stability of the graphite spheroid is reduced at high CE (related to high carbon) and increased Ce/RE contents^{7,25}, conditions where graphite flotation is expected. Furthermore, the eutectic solidification time in a 200x200mm thick section can also increase from about 350 to 500 s when the carbon equivalent is increased from 4 to 4.3%, respectively²⁶. The stability of the precipitating graphite spheroid is also related to how strongly it is coupled to the austenite¹⁶. Here controlled spheroid growth possibly degenerates, by the co-precipitation of austenite, where the nodule is exposed to the melt or to temperature and compositional gradients occurring during flotation of the nodule. Consequently, the key point for Chunky graphite formation is to know what is happening in the last remaining liquid and micro-area around the dendrites during eutectic solidification.

Distribution of Ce in ductile iron

Fascinating insight on the role of Ce and Mg in ductile iron is found in an earlier study²⁵ entailing the radiographic evaluation of a Ce141 isotope in a ductile iron microstructure, from which a number of intriguing observations relating to chunky Graphite formation could be made. In the study, Ce distributes unevenly and preferentially in the grain boundaries of the primary dendrites of austenite²⁵. Here the Ce concentration was about 2 to 5 times higher than in the “ordinary” cast iron microstructure, in which Ce in the metallic phase was 1.5 to 3 times higher than in the graphite phase²⁵. The proposed mechanism for this is as follows²⁵:

1. *Mg is preferentially absorbed on boundaries of growing graphite crystals during cooling and solidification, since Mg is more surface active than Ce with respect to graphite.*
2. *Ce absorbed on the graphite between dendrites (owing to being less horophillic than Mg) is forced back by the growing dendrites of austenite-graphite eutectic, where chemical compounds formation can occur²⁷*
3. *The preferential Mg absorption on graphite crystal boundaries having the lowest reticular density leads to quasispheroidizing of the graphite crystals, owing to that the surface tension coefficients σ_i of select graphite boundaries are levelled in conformity to the Gibbs-Wulff principle ($\sigma_i \rightarrow \sigma'$)²⁵].*

In the above mechanism formation products surrounding the growing dendrites of austenite-graphite eutectic include: compounds like CeFe₅, phases enriched in both Mg and Ce as well as crystallized Mg and Ce that can facilitate Mg₃Ce^{25sic}. It could be that the wide melting range of Ce²⁸ is responsible for the low melting range of many of these compounds of around 800°C that this aggravates the issue. Consequently, it is the formation of compounds rich in Ce and Mg that reduce the concentration of free and surface active Mg below the level necessary to favour the formation of spheroidal graphite^{25sic}. In addition, for Ce based nodulizers it is a clear that chunky graphite prevalence is increased when the oxide content exceeds >10 wt-%²⁹, which fuels the issue about secondary oxidation. Noteworthy is also that Mg and Ce are usually found in formations products like dross, which are often present close to chunky graphite²³. Moreover, since re-melting and wet grinding often precede OES analysis; it is likely that the segregation of Mg and Ce compounds have been elusive. Even if advanced ICP analysis is used it is still difficult to determine a baseline content of Mg and Ce compounds. Perhaps the most striking theme here is the notion of Magnesium's gas-liquid transition with pressure. Here higher pressure than the equilibrium vapour pressure entailed that Mg liquefied, which caused chunky graphite like morphologies^{5,9}. It would seem that the required pressure only involved the interaction of a few atoms at near-solidification temperature^{5,9}, which is less than the about 50 atoms of eutectic composition involved during the eutectic expansion⁹. These conditions are likely to be fulfilled in the thermal centre in heavy castings where solidification times are long and the segregation severe.

Establishing a Cerium baseline to avoid Chunky Graphite in ductile iron

Returning to the aforementioned scenario for small graphite nodules without shells having large growth rates and large interface kinetics¹¹, it could well be that the above segregation of liquefied Mg and/or Ce on the austenite dendrite arms provide ideal conditions for Chunk graphite. Evidence to support this is found in a study on Ce effect on graphite

nodule count and distribution, where excessive Ce concentrations of around 0.02% *promotes the graphite to grow fast* leading to chunky graphite clusters in their microstructures and a drop in nodule count³⁰. Furthermore, in a ductile iron composition with less than 0.5 wt-% Mn, the chunky graphite residual limit for light (Ce rich) and heavy (Y rich) RE alloys were about 0.003 and 0.018 wt-%, respectively in both laboratory and production of a 1.6T component³¹, which corresponded to alloying additions of 0.05 and 0.2 wt-%.

Even if there are numerous studies on different RE additions¹⁵ most other work have centred on Ce additions without primarily focusing on chunky graphite. In the initial patent by Morrogh on “Nodular Cast Irons and The Manufacture Thereof” Ce was paramount to desulfurize and stabilize carbides, but also to ensure sufficient nodularization³². However, if excess Ce is present in the microstructure, Exploded, Spiky and coral Graphite morphologies can be found^{33,34,35}. When the solidification conditions for heavy castings were reproduced by keeping small quantity of molten metal at the eutectic temperature for a long time even the amount of Chunky graphite was increased for Ce contents above 500 ppm together or without increased holding times and/or decreased cooling rates³⁶. In Figure 1 it can be seen that levels below 0.01% (100ppm) Ce could be tolerated if Chunky graphite was to be avoided⁶. However, there are examples where amounts up to 0.02% Ce could be tolerated elsewhere⁷.

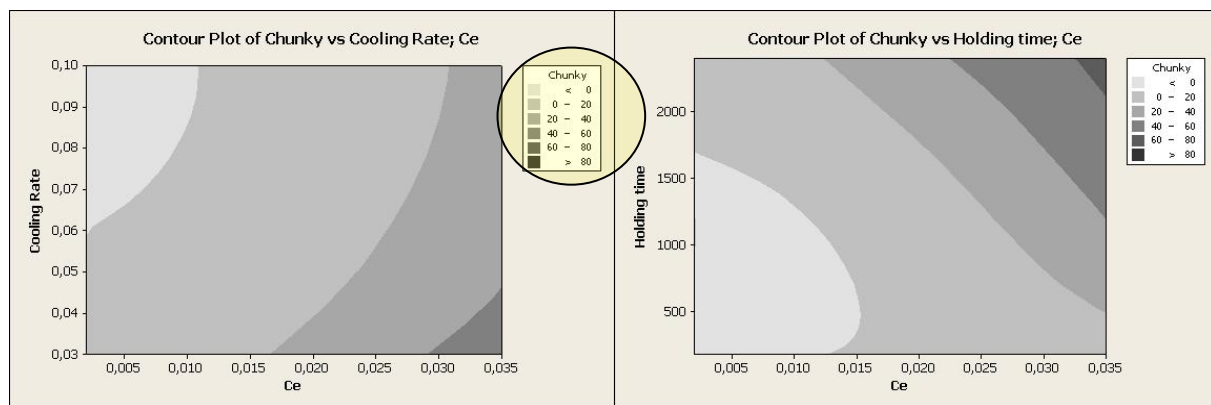


Fig.1: Effect of Cerium, cooling rate (left) and holding time (right) on the amount of chunky graphite. Adapted from⁷

The role of impurities and trace elements

In addition, Mg and Ce with other RE additions in the MgFeSi carrier are primarily used to deal with impurities and trace elements. The RE nodulizer additives whose primary function is to lessen the effect of subversive elements on the melt can be seen in Table 1¹, which can be determined by the graphite denodularization factor, K₁, in equation 2³⁵. Theoretically the denodularization effect can be counteracted with RE (Ce, La, Nd, Pr etc) up to K₁=2. If K₁>1.2 RE addition could be regarded as compulsory, for K₁<1.2 it is beneficial or could be avoided, if a high degree of process control prevails³⁵. This is important when dealing with chunky graphite and clean charges, where the Ce required is often overrated.

$$K_1 = 4,4Ti + 2,0As + 2,4Sn + 5,0Sb + 290Pb + 370Bi + 1,6Al \quad (2)$$

Table 1: Chunky Graphite promoters and their subversive counterparts, adapted from²².

Chunky Promoters	Ce	Ca	Ni	Si	Al	Cu	RE
Subversive counterparts	As	Bi	B	Sb	Sn	Pb	Cu

To limit the impact of RE and Ce on the final microstructure Sb is usually added. In practice, up to 0.005% Sb is used and related to a Sb:Ce ratio between 0.6 and 1.2³⁷, with significantly less Chunky for a ratio higher than 0.8³⁴. Recently, ratios of 2 and above have been used in a theoretical study where the RE content was in excess of 2.5% in the nodulizer³⁸. Here Sb acts like a diffusion barrier around the graphite⁸ and leads to higher nodularity and nodule counts, but it is obvious that the mechanism involved with Sb addition needs to be studied further. Especially since required the thickness of the diffusion barrier is stated as between till 1nm and 4nm^{8,39} and the interaction with Ce and other RE is unclear.

The role of sulphur and magnesium

Fortunately, the chemical stability and availability of free Mg has received greater interest amongst the scientific community. Here issues governing availability and segregation of Mg are important. These include: secondary

oxidation during pouring, reaction with refractory, the evaporation/fading out of Mg gas bubbles and Mg segregation at the austenite-residual melt interface^{5,9}. For the purpose of controlling the Mg-treatment the availability of free Mg and avoiding bound Mg related to inclusions is easiest. In practice oxygen, sulphur and trace elements need to be controlled to achieve a stable Mg-treatment process. Owing to S and O being surface active elements these will boost prism plane growth of the graphite leading to laminar and chunky graphite morphologies. However, if S, O, other surface active elements and trace elements are controlled the basal plane will be favoured, which favours nodular morphologies.

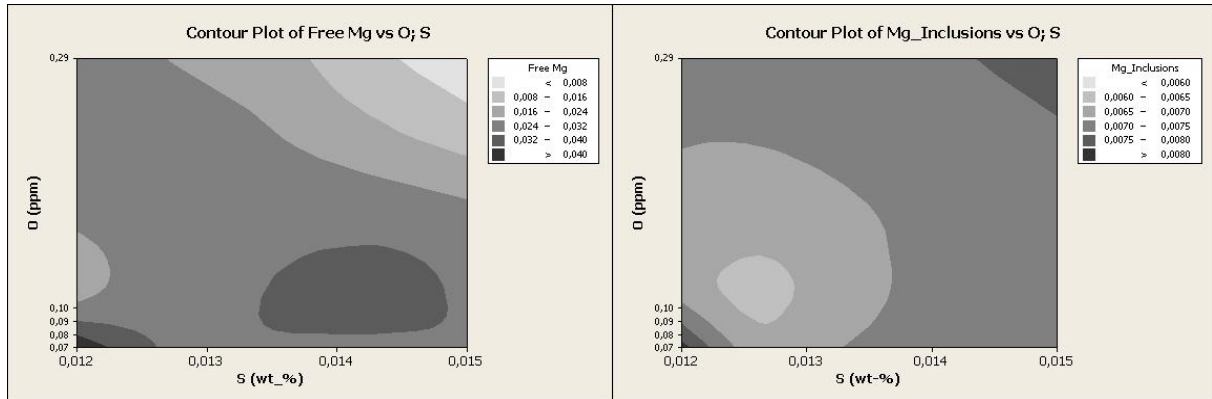


Fig.2: Optimum S, O and Mg levels in the Mg-treatment of ductile iron. Adapted from¹⁶

Unfortunately, it is only possible to distinguish between free and bound magnesium with advanced characterization methods like Inductively Coupled Plasma, ICP¹⁶. These are elucidated in Figure 2¹⁶ where it is seen that high amounts of S and O should be avoided, since excessive 0.05wt-% Mg amounts can favour the degeneration of graphite and increase the amount of intercellular carbide³⁵. Regardless of total magnesium content, the bound content Magnesium has been determined to about 0.006 and 0.008 Wt-% Mg,¹⁶ possibly due to few data points and a clean charge. In the same study it was more useful to look at O and S separately with the Mg-content. Here it was found that $0.012 < S < 0.013$, $0 < O < 0.2$ ppm and $0.035 < Mg < 0.045$ seem to be good interval to conduct the Mg-treatment in¹⁶. Generally 0.005 to 0.015wt-% S is beneficial to control Mg-treatment recovery, nodular graphite nucleation and the formation of inclusions³⁵. Furthermore 0.0137 Wt-% S was found to minimize chill formation in the final microstructure of thin 2 mm strips⁴⁰. The same study also found that Mg/s ratio >0.76 was necessary to ensure that nodularity was at least 80%. Moreover, reducing the Mg content in the Mg-alloy from 6% to 3% lead to higher solidification temperatures and lower amount of chill⁴¹. Furthermore, during the last decade, significant progress has identified an even narrower sulphur content range from 0.008 to 0.012 wt% S. Low Sulphur levels (<0.005 wt% S) increased the risk of exploded graphite and high Sulphur levels (>0.0135 wt% S) increased the risk of compacted graphite⁶. Here it was the Mg-rich inclusions in the graphite nucleus that lowered nodularity, either through a de-nodulizing hexagonal structure or due to the size of the S rich nucleus getting too big. Furthermore, the development of the oxygen activity meter has now made it possible to measure the transition between different graphite types. For example the transition from compacted graphite, CGI, to lamellar graphite, LG, could be delayed by a factor of 5 if the S content was reduced from 0.0135 to 0.008 wt% S⁴². Hopefully this could be applied and reduce the likelihood for chunky graphite formation.

The increasing importance of surface tension

In fact, it is here that the surface tension of the liquid-graphite interface is receiving particular research focus today. The main obstacle so far is the complex chemistry, undefined interactions and oxidation potential of different elements in cast iron. Nevertheless, important relationships between temperature, surface tension and oxygen activity are beginning to emerge⁴³. Moreover sensor technology is rapidly evolving to facilitate accurate measurement of temperature, surface tension and oxygen activity. It could be postulated that their concurrent measurement is what is needed to gain important insight in the control of the ductile iron production process. In particular key processes like liquid state after melting, extent of super heating, control of the nodularization treatment and the tailoring of the inoculation process are those that likely to benefit most from implementing sensor technology.

Today particular surface tension values are available^{44,45} to demonstrate that it is possible to use surface tension to distinguish between different graphite forms. Below around 900-990 mN/m flake graphite occurs^{44,45}. The vermicular region has been estimated to be between 1082 and 1360 mN/m⁴⁵. The nodular region has been estimated at above 1465 mN/m⁴⁵. Unfortunately, the reported surface tensions values for the intermediate vermicular and nodular transitions vary too much between researchers to be conclusive. The reason for this is that experimental conditions and the equipment have little resemblance to each other. Furthermore, the chemistries of the melts are inconsistent due to natural variation of the raw materials in terms of e.g. oxygen content. Another issue is that the content of surface active elements like Mg, Ce, Ba etc are different.

Conclusions

From the review a number of interesting observations could be made:

1. Under certain conditions sulphides could be a poor nucleant for graphite, but a good one for silicates that are with proper treatment and inoculation good nucleation sites for graphite
2. Ce distributes unevenly and preferentially in the grain boundaries of the primary dendrites of austenite
3. Ce concentrations of around 0.02% *promotes the graphite to grow fast* leading to chunky graphite clusters
4. Sulphur is very important for the graphite morphology in ductile iron

References

1. P. C. Liu, C. L. Li, D. H. Wu and C. R. Loper Jr.. AFS Transactions. 1983, Vol 91 No 83-51 pp. 119-126.
2. B. Prinz, et al. Giessereiforschung, 1991, Vol. 43, No. 3, pp. 107-115
3. J. Zhou, W. Schmitz and S. Engler. Giessereiforschung, 1987, Vol. 39, No. 2, pp. 55-70
4. M. Gagné and D. Argo: Proc. Int Conf. on Advanced Casting Technology, Kalamazoo, Michigan, USA, 12-14 Nov, 1989, ASM Int. pp231-256
5. H. Itofuji. AFS Transactions 1996, Vol 104 No 96-131 pp. 79-87.
6. Shoji Kiguchi; Masayuki Sintani; Haruyoshi Sumimoto and Kokichi Nakamura. Journal of Japan Foundry Engineering Society. 2000, Vol. 72, No. 5, p.311-316.
7. A. Javaid and C. R. Loper Jr. AFS Transactions 1995, Vol. 101 No 95-49 pp. 135-150.
8. W. C. Johnson and B. V. Kovacs, Metallurgical and Materials Transactions A, 1978, Vol. 9 (2), pp. 219-229.
9. H. Itofuji, H. Uchikawa, AFS Transactions 1990, Vol. 98 No 90-42 pp. 429-448.
10. H. Nakae and Y. Igarashi, Materials Transactions, 2002, Vol. 43 (11), pp. 2826-2831
11. H. Fredriksson, J. Stjern Dahl and J. Tinoco. Mat. Sci. Eng. A 413 (2005) pp. 363-372
12. S. Lekakh and C. R. Loper Jr. AFS Transactions 2003, Vol 111 No 03-103(05) pp. 885-894.
13. T. Skaland, A model for graphite formation in Ductile Cast Iron, PhD thesis. NTH 1992:33
14. Y. Igarashi and S. Okada. Journal of Japan Foundry Engineering Society. 1998, Vol. 70, No. 5, p.329-335
15. T Skaland. Nucleation Mechanisms in Ductile Iron. Proceedings of the AFS Cast Iron Inoculation Conference, American Foundry Society (AFS), Schaumburg, Illinois, 2005, Sept. 29-30, pp. 13-30
16. H. Itofuji. Journal of Japan Foundry Engineering Society. 2000, Vol. 72, No. 10, p.645-651 .
17. H. Itofuji and A. Masutani.. Journal of Japan Foundry Engineering Society. 2004, Vol. 76, No. 2, p.98-106 .
18. H. Itofuji and A. Masutani. International Journal of Cast Metals Research (UK). 2001, Vol. 14, No. 1, pp. 1-14.
19. K. Hanawa, K. Akechi, Z. Hara and T. Nakagawa,. Trans. J. Inst. of Metals, 1980, Vol.21 (12) pp. 765-772
20. W. Khraisat, H. Borgström, L. Nyborg, and W. A. Jadayil, Powder. Metall., 2009 Vol. 52 (4), pp. 291-29
21. A. Udriou. Giesseri Rundschau 60 Heft 11/12 pp. 356-374
22. S-E. Wetterfall, H. Fredriksson and M. Hillert J. Iron Steel Inst. (1972) pp. 323-333
23. R. Källbom, K. Hamberg, M. Wessén and L.-E. Björkegren. Mat. Sci. and Eng. A, 2005, Vol. 413, pp. 346-351
24. H. Fredriksson Mat. Sci. Eng. 65 (1984) pp 137-144
25. V. A. Guiva, A. P. Lyubchenko and M. V. Mozharov Met. Sci. and Heat Treat., 1970, Vol. 12 (12), pp. 994-997
26. T. Kanno, I. Kang, Y. Fukuda, T. Mizuki and S. Kiguchi. Effect of Pouring Temperature and Composition on shrinkage Cavity in Sheroidal Graphite Cast Iron. AFS Transactions 2006, Vol 112 No 06-084 pp. 525-534.
27. H. F. Fischmeister, A. D. Ozerskii and L. Olsson, Powder Metallurgy, 1982, Vol. 25 (1), pp. 1-9
28. Melting temp. 795°C & Boiling temp. 3257°C: www.chemicalelements.com/elements/Ce.html Accessed 2011-05-12
29. H. Löblich 2006, Giessereiforschung, Vol 58, No.3 pp. 2-11.

10th International Symposium on the Science and Processing of Cast Iron – SPC110

30. X. Diao et al. *Int. J. Modern Physics B* Vol. 23, No 6 & 7 (2009) pp 1853-1860
31. Y. Niu and Z. Zhang *Foundryman*. 1988 Vol. 81 (8), pp. 390-398.
32. H. Morrogh, Nodular cast iron and the manufacture thereof. US Patent 2488511, Nov. 15th, 1949
33. C. R. Loper Jr. and K. Fang. *AFS Transactions* 2008, Vol. 114 No 08-066(05) pp. 673-682.
34. P. Larrañaga, et al. *Metallurgical and Materials Transactions A*, 2009, Vol. 40, No. 3, pp. 654-661.
35. I. Risposan, M. Chisamera and S. Stan. *China Foundry*, 2010, Vol 7 No. 2 pp. 163-170
36. S. Méndez, et al. Experimental Investigation of Chunky Graphite Formation in Small-Section Ductile Iron Castings. Proc. of 69th World Foundry Congress, Hangzhou China 2010, Oct. 16-20, pp. 0387-0392
37. Rio Tinto Iron & Ti.. *Chunk Graphite Defects in ductile Iron*. The Sorelmetal Book of Ductile Iron, 2006 p 93
38. L. Zhe, C. Weiping and D. Yu, *China Foundry*, 2012, Vol. 9 No. 2 pp. 114-118
39. B. Kovacs, Method for Increasing Mechanical Properties In Ductile Iron by Alloy Additions. United States Patent 4363661, Dec 14th, 1982
40. Y. Igarashi and H. Nakae. *Journal of Japan Foundry Engineering Society*. 2002, Vol. 74, No. 1, p.30-35 .
41. H. Nagayoshi and K. Imanishi. *J. J. Foundry Engineering Society*. 1996, Vol. 68, No. 8, p.631-636 .
42. F. Mampaey, D. Habets, J. Plessers and F. Seutens, *Int. J. of Metalcasting*, 2010, Vol. 4 (2), Pp 25-43
43. K. Morohoshi, M. Uchikoshi, M. Isshiki and H. Fukuyam *ISIJ International*, 2011, Vol. 51 (10), Pp. 1580-1586
44. G. Paul, *Journal of the Southern African Institute of Mining and Metallurgy*, 1972, Vol. 72(1), pp. 165-170
45. D. Shi, D. Li, G. Gao and L. Wang, *Materials Transactions*, 2008 Vol. 49 (9), pp. 2163 to 2165